Three-dimensional magnetic resonance microscopy of pulmonary solitary tumors in transgenic mice

M. Takahashi[1], S. Kubo[1], E. Levantini[2], S. Kobayashi[2], O. Kocher[3], D. G. Tenen[2]

[1]Radiology, Beth Israel Deaconess Medical Center, Boston, MA, United States, [2]Hematology/Oncology, Beth Israel Deaconess Medical Center, Boston, MA, United States, [3]Pathology, Beth Israel Deaconess Medical Center, Boston, MA, United States

Introduction

The field of cancer modeling in mice is progressing at an accelerating pace to create mouse models that accurately reproduce the genetic and histopathological alterations present in human tumors [1]. This has highlighted the need to follow the temporal and spatial patterns of pulmonary solitary tumor progression in small rodents. Thus, establishment of a noninvasive method is imperative for investigating or monitoring the lesions, and for evaluation of therapy response. In the present study, we attempted accurate detection of pulmonary solitary tumors as well as other complicated pulmonary disorders in aging inbred transgenic mice by magnetic resonance (MR) microscopy at 4.7 Tesla.

Materials and Methods

We used 17 transgenic mice of mixed background (c57b6-129-FVB/N, ranging 9-17 months of age). All animals were anesthetized with 1.5-2% isoflurane (IsoFlo®, Abbot Laboratories, North Chicago, IL) via a nose cone for *in vivo* MR microscopy. All Micro-MRI protocols (I – III) mentioned bellow were adapted for operation at 4.7 Tesla (Biospec 47/40, Bruker BioSpin, Karlsruhe, Germany) with synchronized cardiac-respiratory gating such that the MR signal was acquired at each cardiac phase and at end-expiratory phase. Each animal was intravenously injected with a macro-molecule MR contrast agent (Gd-DTPA-BSA, provided by EPIX, Cambridge, MA) at a dose of 0.1 mmol Gd/kg prior to MRI. We have imaged the animals with following protocols: (I) Two-dimensional (2D) multi-slice gradient echo imaging (screening) was performed in transverse and coronal planes encompassing the entire lung. A TR was selected less than the duration of one cardiac cycle (ca. 180 msec), where one k-space line was filled for each image per single heartbeat. Other scan parameters were: minimum TE (1.8 msec), flip angle = 22º, matrix size = 256 × 256, FOV = 2.56 cm^2, slice thickness = 1 mm, and NEX = 4. (II) Based on the MR screening results, we selected the mice with pulmonary solitary tumors. T1WI and T2WI were conducted in image slabs depicting the tumors using a conventional spin echo (TR/TE=500/11 msec) and fast spin echo sequences (TR/TE=2000/31 msec). Other scan parameters were: matrix size = 256 × 256, FOV = 2.56 cm^2, slice thickness = 1 mm, and NEX = 4. (III) All mice with solitary tumors were additionally subjected to a 3D gradient echo sequence. TR and TE were the same those used in the screening and the other scan parameters were: FOV = 2.56 × 2.56 × 2 cm^3, matrix size = 128 x 128 x 100 (zerofilled to 128 x 128 x 128) and NEX = 1, affording a (200 μm^3) isotropic voxel. Total scan times were approximately 6-7 minutes (I), 8 and 4.4 minutes (II), and 1.1 hours (III), depending on the individual animal's cardiac/respiratory rates. On 2D images, we measured the size of the tumor in longitudinal and short axes. Further, the 3D datasets were processed and analyzed in each animal as follows: The first step involved the isolation of the lung using a semiautomatic segmentation method based on a finite snake algorithm. The VOI isolated in this manner was then computed to generate both maximum intensity projections (MIP) and volume rendered (VR) images using ImageJ (ver. 1.33) and Insight SNAP. After the imaging session, the lungs were inflation-fixed with 2.5 ml of 10% formalin, then histologically evaluated in 10-12 µm sections which corresponded to the axial MR image slabs. The protocols for this study were approved by the Institutional Animal Care and Use Committee.

Results and Discussion

Twelve out 17 mice revealed several types of pulmonary disorders (total of 25 abnormalities), including 7 solitary masses, which were histologically validated. Six of 7 solitary masses were adenocarcinoma, which is the most common form of lung carcinoma, responsible for nearly half of non-small-cell lung cancer cases. By *in vivo* screening (I), most of these abnormalities were identified, and the correlation with histological findings was over 95%. Furthermore, a very small (< 1 mm) tumor was detected. In the subsequently performed 2D spin echo imaging of mice with solitary tumors, both T1 and T2 weighted imaging provided higher image contrast than the gradient echo screening, so that the tumors could be distinguished from the surrounding complications such as edema or atelectasis (Fig. 1). On the 3D gradient-echo images (200 µm isotropic voxel), the tumors could be observed in any direction, which allowed tracing of the pulmonary vessels and the delineation of solitary tumors. The generated MIP and VR images on the 3D datasets allowed the viewers to grasp the spatial location of solitary tumors relative to the orientation of the pulmonary vessels (Fig. 2). The volume of each tumor could also be measured (ranging: 1.5 - 680 mm^3).

In summary, these results offer the promise of *in vivo* MR microscopic assessment of pulmonary solitary tumors in transgenic mice. The stepwise protocols demonstrated in the present study can be utilized to design further MRI studies in small animals for better understanding of progression of solitary pulmonary tumors or responsiveness to particular therapies.

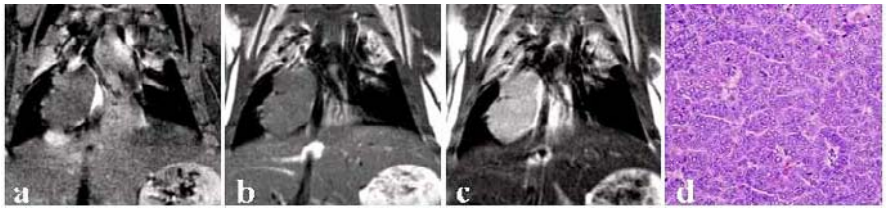

Fig. 1. Typical MR images (a – c) and microphotograph (d) of pulmonary solitary tumor (adenocarcinoma) found in transgenic mouse. a) gradient echo image; b) T1 weighted spin echo image; c) T2 weighted spin echo image.

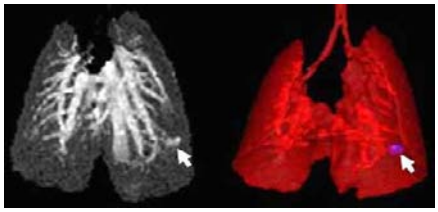

Fig. 2. Maximum intensity projection (MIP, left) and volume rendered (VR) images (right) of the lung in a mouse with small tumor (arrow: adenocarcinoma, 0.6 mm x 1.5 mm) in the right lower lobe. The images were posterior view and the VR image (right) has high transparency to exhibit the tumor.

Reference: 1. Meuwissen R, Berns A, Genes and Development 19 (2005) 643-664.